DETECTION OF RISING DAMP AND MATERIAL CHANGES ON HYPERBOLOID COOLING TOWER SHELLS BASED ON THE INTENSITY OF THE REFLECTED LASER BEAM

Maria Makuch

Summary

Using a hyperboloidal cooling tower undergoing repair as an example, the paper examines the possibility of using a laser beam reflectance intensity value for the automated detection of perforations in cooling tower shells and the identification of material changes characteristic of the renovated sections of reinforced concrete structures. Due to the specific geometry of the analysed object, the practical application of the value of the fourth coordinate was preceded by its a priori modification. The applied correction solution made it possible to effectively eliminate the influence of the measurement geometry, adjusting the intensity values to correspond to the properties of the scanned surface. In the usability analyses of the corrected radiometric data, the author's approach to eliminating information loss was applied, assuming the use of the fourth coordinate values as scalar fields. The proposed methodology was verified by comparing the obtained results with those of the commonly used unsupervised classification. The agreement, based on the similarity of the structures, between the results of the image classification and the areas extracted through the segmentation of the scalar fields, representing the corrected values of the laser beam reflectance intensity, confirmed the reliability of the proposed solutions. The usefulness of the radiometric data in 3D space was confirmed by comparing the obtained results with the analyses of the local surface curvature determined by the point cloud based on principal component analysis. Thanks to the segmentation of the scalar fields, the detection of rising damp and corrosion leaks, consistent with the results of the surface condition assessment based on the local curvature analysis, made it possible to specify the degree of degradation of the hyperboloid shell according to a seven-point scale that is consistent with the industry requirements. The values of the fourth coordinate also allowed the identification of material changes caused by the repair, and their comparison with the shell damage contours extracted from the local curvature analysis made it possible to verify the amount of repair mortar used and to assess the validity of the work carried out.

Keywords

intensity • point cloud • unsupervised classification • terrestrial laser scanning (TLS) • non-destructive testing (NDT) • intensity correction

1. Introduction

1.1. Problem Statement

Hyperboloid cooling towers are distinctive tower structures designed to cool industrial waters by discharging their heat into the ambient air [Bamu and Zingoni 2005]. The most common group of cooling towers in use in the Polish industry are structures erected in the second half of the last century. Extremely economical design, poor quality of materials and faulty workmanship of these thin-walled structures, overloaded during many years of use with unfavourable operating conditions and the influence of an industrial atmosphere with increased aggressiveness, determine their continuing degradation. The most important external phenomenon prompting the repair of exploited cooling towers is the loss of the protective capacity of the concrete lagging, manifested by cavities and chipping of the concrete, as well as perforations of the shell with seeping moisture [Jawański and Stefanek 2011, Zacharopoulou et al. 2013]. The economic consequences of the decommissioning of the cooling tower, involving the need to stop technological processes, force periodic repair measures to be taken, adapted to the condition of the hyperboloid structure.

The basis for monitoring and designing appropriate repair programmes is diagnostic work, which most often comes down to direct visual examination, carried out with the support of optical tools [Makuch 2018]. The registration of defects found on several hundred metres long monolithic cooling tower shells, with no permanent and clear identification marks, is a particularly labour-intensive and arduous task [Antoniszyn et al. 2016]. With the development of new measurement technologies, including terrestrial laser scanning (TLS), there is a growing acceptance of remote non-destructive testing (NDT) methods in modern engineering structure diagnostics. Terrestrial laser scanners enable the non-contact and automatic measurement of the spatial coordinates of millions of points, in near real-time [Mills and Barber 2003]. TLS technology provides a complete, three-dimensional record of an object's condition [Olsen et al. 2009], solving the problem of subjectivity in visual assessment [Mosalam et al. 2014], prevents missing important information [Chen 2012] and removes the space for arbitrary interpretation of reports and generalised inspection results [Anil et al. 2013]. Also, noteworthy is the non-intrusive nature of laser scanning that allows inspections to be carried out without interfering the facility operations, reducing the need for skilled manpower [Erkal and Hajjar 2017, Chen 2012]. Additionally, the reach of TLS technology means that there is no need for the typically used suspended scaffolding [Laefer et al. 2010].

The main application of scanning instruments in the assessment of the condition of cooling tower shells is the monitoring of deformation [Ioannidis et al. 2006, Kocierz et al. 2016, Gradka and Kwinta 2017, Kwinta and Bac-Bronowicz 2021]. Often, a detailed 3D model of the structure, based on point cloud data obtained by the scanner, serves as a reference for other types of data, such as digital photos [Piot and Lançon 2012, Camp et al. 2013]. In addition to geometric information, the intensity of the laser beam reflectance, referred to as the fourth coordinate, is also recorded at each point of the cloud. Data regarding the strength (intensity) of the returning signal reflected from

the scanned surface is an increasingly used parameter in the assessment of structural conditions [Tsai and Li 2012, Xu et al. 2015]. The relationship between the value of the fourth coordinate and material features of the scanned surface, influenced by colour [Voegtle et al. 2008], roughness [Krooks et al. 2013], and dampness [González-Jorge et al. 2012], allows the classification and segmentation of the investigated surface based on its diverse properties [Armesto-González et al. 2010, Crespo et al. 2010, Zaczek--Peplinska et al. 2012].

In this article, the possibility of adopting the intensity values of the laser beam reflectance for the automated detection of perforations in cooling tower shells and the identification of material changes characteristic of the renovated sections of reinforced concrete structures is demonstrated, using a hyperboloidal cooling tower shell undergoing repair as an example. Based on data acquired by a terrestrial laser scanner, defining two states of the hyperboloidal shell (before and after repair), a solution has been proposed for the inspection of shell damage caused by moisture infiltration (accompanied by visible stains and streaks on the surface) and the monitoring of repair operations (ensuring control over the quantity of repair mortar used). This complements the considerations based on the analysis of the local curvature of the cooling tower shell, as detailed in the work [Makuch and Gawronek 2020].

1.2. Related studies

Radiometric TLS data, defined by laser beam reflectance intensity values, are successfully used in surface condition diagnostics. The relationship between the intensity of reflected radiation and the nature of the scanned surface, its colour, roughness, and moisture content consistently stimulates research. The literature provides numerous case studies showcasing the use of the fourth coordinate values in the detection of cracks and fissures [Xu et al. 2015], excessive rising damp [González-Jorge et al. 2012], material changes [Hancock et al. 2012, Gawronek and Noszczyk 2023], or biological damage [Toś 2013].

The solutions based on raster classification of intensity measurement results using automatic image recognition techniques are particularly popular in assessing surface conditions. This approach, mainly employed in monitoring the state of historical architecture, appeared first in the work of Armesto-González et al. [2010], who demonstrated that radiometric TLS data can be used in evaluating the condition of the facade of a historic building. Two-dimensional intensity reflectance images generated from the point cloud were subject to unsupervised classification, which created groups of pixels with similar radiation reflectance properties. The obtained results, verified by expert assessment, confirmed the effectiveness of the adopted methodology, especially in detecting excessive damp often correlated with micro-damages to the surface. Similarly, Crespo et al. [2010], García-Talegón et al. [2015], and Gawronek and Noszczyk [2023] analysed the usefulness of laser beam reflectance intensity in detecting damage as well as rising damp and material changes on historic facades. The unsupervised classifications of intensity images present in these works allowed for an

effective characterisation of surface changes, providing both quantitative and qualitative information. In the work of Li and Cheng [2018], unsupervised classification of a raster representation corrected for intensity values was employed to detect damage inside an ancient building. The proposed correction models made intensity data more representative of the scanned surface properties, thereby improving the effectiveness of this approach in assessing the condition of the interiors of historic buildings.

Many scientific papers investigating the usefulness of laser beam reflectance intensity values have also been dedicated to the analysis of the condition of engineering objects. The paper by Zaczek-Peplinska et al. [2012] presents an analysis of the potential application of radiometric data classification, obtained by a ground laser scanner, in the assessment of the ageing water dam. The results obtained from laboratory and field studies allowed a positive evaluation of the proposed approach, especially in assessing the dampness of external layers of concrete, essential for the detection of filtration phenomena. Meanwhile, González-Jorge et al. [2012], based on the classification of laser beam reflectance intensity values, assess the degree of dampness in the concrete pillars of a bridge and detect vegetation efflorescence, indicating problems with high surface porosity that increase water infiltration leading to structural degradation. The proposed method provided reliable (quantitative and qualitative) information regarding the condition of the bridge's concrete pillars, with higher efficiency and detail than traditional visual assessments. Similarly, Toś [2013] analysed the usefulness of laser beam reflectance intensity in detecting dampness, salt efflorescence, and plant succession on flood embankments. The research used digital image analysis techniques, with supervised classification of data obtained by two laser scanners operating at different wavelengths. In both cases, adverse phenomena occurring on the analysed surface were effectively identified. The presented method was considered an alternative to the traditional way of cataloguing damage based on visual assessment and surface conditioning with the support of expert opinion.

Despite the high popularity of solutions based on raster classification of laser beam reflectance intensity values, the research literature also contains applications that use radiometric information acquired directly from point clouds. Hancock et al. [2012] present one such approach, using the intensity value of laser beam reflectance to assess the damage caused by fire to a concrete structure. Preliminary results from a laboratory study on concrete blocks were promising, indicating the possibility of determining the temperature that affected individual elements of the structure based on the fourth coordinate value. Mukupa et al. [2016] confirm that it is feasible and reasonable to rely on laser beam reflectance intensity information when assessing the durability of fire-damaged concrete structures. They point out the superiority of TLS technology over traditional methods, emphasising that remote assessment of the condition of a fire-damaged structure with a ground laser scanner will improve the safety of diagnostic work, replacing traditional visual methods and enabling accurate assessments of the need to reinforce specific elements that have lost load-bearing capacity due to high temperatures. Similarly, Lerones et al. [2016] successfully utilised laser beam reflectance intensity information in the detection of rising damp in historic buildings based on point cloud data. The obtained results allowed a positive assessment of the

TLS-based approach, providing comprehensive 3D information on the damage caused by excessive dampness. Meanwhile, Buczek et al. [2017], based on radiometric data acquired by a ground laser scanner, proposed a solution dedicated to recognising rock layers in geological cross-sections. Using intensity value histograms and calibration samples in a fully automated way, they analysed the stratification of two mine deposits. The consistency of the results of the intensity distribution analyses with the rock types determined by geologists confirmed the superiority of the proposed metric solution over subjective and imprecise traditional methods.

While the intensity value of the laser beam reflectance is considered to be an important source of spectral information that provides reliable data about the properties of the scanned surface, the limitations of this approach cannot be overlooked due to the influence of other factors that determine the value of the fourth coordinate. The intensity of the reflected signal detected by the TLS instrument is strongly correlated not only with the properties of the scanned surface but also with variables such as instrumental, atmospheric, and methodological factors [Kaasalainen et al. 2011]. In the case of measuring homogeneous surfaces with the same scanning device under unchanged measurement conditions, the beam incidence angle and the scanner-object distance are the key factors for the quality of the obtained fourth coordinate value [Soudarissanane et al. 2011]. Most of the discussed case studies concern plane-like objects, and the analyses presented are limited to test fields located opposite the scanning instrument, using original (uncorrected) values of the fourth coordinate. However, such a measurement methodology cannot be maintained in the case of the analysis of the hyperboloidal shell of a cooling tower located in an industrial plant. Due to the specificity of the analysed object, in this paper, the practical application of the fourth coordinate value was preceded by its a priori modification. The purpose of the intensity correction is to transform it into a value proportional or equal to the value associated with the properties of the scanned surface. In the analyses of the utility of corrected radiometric data for the detection of perforations in the cooling tower shell and the identification of material changes in renovated fragments of a reinforced concrete structure, an original approach was used to eliminate information losses (resulting from the conversion of 3D data into 2D images). This approach involved the segmentation of scalar fields, representing normalised and corrected laser beam reflectance intensity values. The obtained results were compared with the outcomes of commonly used unsupervised classification and with the surface damage of the hyperboloidal cooling tower shell that was extracted based on local curvature analysis.

2. Materials and methods

2.1. Test cooling tower and data acquisition

The research object (Fig. 1) is a hyperboloidal cooling tower, built in the second half of the 20th century, located on the premises of the historic Tadeusz Sendzimir Steelworks. The reinforced concrete shell of the cooling tower has the shape of a rotational hyperboloid with a thickness of 0.4 m–0.12 m. The height of the thin-walled structure,

measured from the ground surface, is 65 m, with a horizontal diameter of 43 m at the lower ring and 27 m at the crown. Due to extensive corrosive damage to the reinforced concrete shell and ageing after a long period of operation, the structure required repair and, therefore, appropriate research.
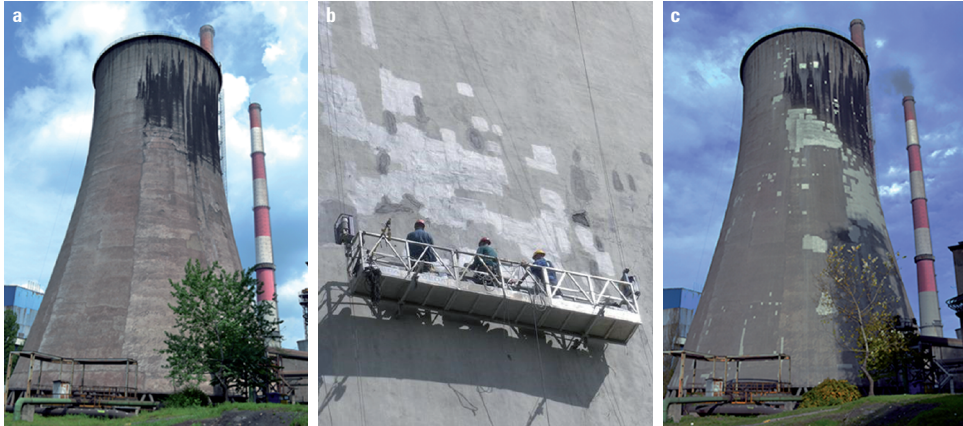
Source: Author's own study

Fig. 1. The research object and its repair: **a.** cooling tower before repair; **b.** repair of the outer shell; **c.** cooling tower after repair

The pre-repair technical assessment, based on indirect (from the ground, using binoculars with tenfold magnification) and direct (in collaboration with a team of climbers whose activities were coordinated from the ground) visual inspection of the cooling tower shell, identified varying degrees of corrosion damage, including shell perforations with moisture seepage. The repair work included designing a localised replacement of concrete detached from the structure, the removal of shell perforations, and reprofiling of local defects in the cover by the application of appropriate repair mortars.

Ground-based laser scanning of the test cooling tower was performed twice (before and after the repair of the shell) using the Z+F Imager 5010 phase-based instrument from nine measurement positions situated around the structure. Periodic observations of the object were made in relation to a stable observation network and its associated reference system. The positioning of the instrument was the result of optimising the TLS data acquisition for the entire shell while maintaining the correct measurement geometry. The observation network, securing the positions of the measurement stations and reference points, ensured the consistency of the measurement procedures and minimised factors differentiating the data obtained in each series. The adopted measurement methodology involved placing the scanner at positions with known coordinates and referencing it to clearly identifiable reference objects in the point cloud (black-and-white target discs and steel reference spheres).

2.2. Intensity correction and normalisation

The general relationship between the signal power emitted by a ground-based laser scanner (P_E) and the intensity of the received signal (P_R) is described by the so-called *laser equation* [Suchocki et al. 2016]. Given that the scanned surface is Lambertian surface, the return signal power is determined from the following [Pfeifer et al. 2007]:

$$P_R = \frac{\pi P_E \, \rho \, \cos\theta}{4R^2} \eta_{Atm} \eta_{Sys}$$

(1)

where:

   ρ – a coefficient defining the properties of the scanned surface,
   θ – incidence angle of the laser beam (^{g}),
   R – distance between instrument and scanned object (m),
   η_{Sys} – system coefficient (instrumental),
   η_{Atm} – atmosphere coefficient.

The resolution and range of the fourth coordinate value are determined by the type of rangefinder, laser wavelength, transmitter power, filters used, and detector sensitivity. By conducting successive measurement campaigns with the same instrument, the instrumental coefficient (constrained by the technical specification of the laser scanner) could be assumed as a constant and unchanging value [Fang et al. 2014]. Meanwhile, the influence of the atmosphere coefficient, assuming the constancy of the measurement conditions (temperature, pressure, and air humidity) and the limited range of the phase scanners, was accepted at a unity level [Franceschi et al. 2009]. The laser equation was reduced to a form containing an unknown but constant value for the Z+F 5010 instrument, denoted as C_E [Tan and Cheng 2016]:

$$C_E = \frac{\pi P_E \, \eta_{Sys}}{4}$$

(2)

Based on (1) and (2), the intensity of the received signal was defined as:

$$P_R = \frac{C_E \, \rho \, \cos\theta}{R^2}$$

(3)

Assuming a constant instrumental effect and the insignificance of the influence of the atmosphere coefficient, the usefulness of the fourth coordinate value in analyses of the scanned surface properties required the elimination of the impact of measurement geometry coefficients [Humair et al. 2015], described by two parameters: the distance between the scanner and the scanned object (R) and the incidence angle of laser beam (θ) [Soudarissanane et al. 2011]. Increasing the distances significantly reduces the value of the fourth coordinate (I) [Blaskow and Schneider 2014]. Similarly, an increase in the incidence angle of the laser beam reduces the amount of energy returned to the instrument, confirming theoretical assumptions derived from Lambert's law [Kaasalainen et al. 2011]. In the subject literature, multiple attempts have been made to model the

influence of measurement geometry on laser beam reflectance intensities [Tan and Cheng 2016, Humair et al. 2015, Fang et al. 2014, Krooks et al. 2013, Kaasalainen et al. 2011], indicating the possibility of excluding them from radiometric data using appropriate correction functions based on the dependencies $I(R, α, ρ)$, specified by the laser equation [Kashani et al. 2015].

The distance (R) between the scanner and the observed object affects the value of the fourth coordinate in a way that mainly depends on the technical specifications of the instrument. Considering the inverse proportionality of the fourth coordinate value to the square of the distance, in most cases, proves to be an effective method of modifying radiometric data [Fang et al. 2014, Humair et al. 2015]. In the Z+F scanners, the excessive influence of the detector on the variability of intensity values is clearly noticeable at short distances (up to 10–15 m), where the fourth coordinate value deviates significantly from the dependencies described by the laser equation, necessitating the estimation of additional parameters to reduce the so-called *near-range effect* [Fang et al. 2014]. The geometry employed in measuring the research object (deliberate lengths > 15 m) meant there was no need for *the near-range effect* correction parameter.

The ratio of intensity values and the cosine of the laser beam incidence angle (θ) described by the laser equation has also been successfully applied to modify the values of the fourth coordinate [Humair et al. 2015]. The influence of the incidence angle of the laser beam is particularly conditioned by the scattering properties of the object [Kaasalainen et al. 2011]. Taking into account the properties of the scanned surfaces (ρ), which tend to modify the applied Lambertian reflectance model in the laser equation (suitable for perfectly diffusing surfaces), is especially important for rough surfaces where an additional parameter $k < 1$ is applied to correct the value of the angle θ (for example, $k = 0.6$ for a rocky mountainside) [Humair et al. 2015]. The correction of the intensity of the research material was performed assuming that the reinforced concrete shell of the cooling tower approximately satisfies the roughness criterion, characterised by scattered reflection in accordance with *Lambert's law* [Tan and Cheng 2016, Suchocki et al. 2016].

The corrected value of the fourth coordinate (I_c) for the i-th point of the point cloud, defined as a function of distance (R_i) and the laser beam incidence angle (θ$_i$), was determined as the product of the intensity value (I) and the inverse of the relationship in the laser equation [Humair et al. 2015]:

$$I_C\left(\rho\right) = \frac{R_i^2}{\cos\theta_i} \tag{4}$$

The solution based on the relationships described by the laser equation (1), assuming the constancy of the atmospheric and instrumental conditions (C_E = constant), provided a relative and comparable value of the fourth coordinate, reducing its variability resulting from measurement geometry. The intensity correction value for the distance R_i (for the i-th point of the point cloud) was determined based on the spatial coordinate differences between the scanner centre and the i-th point [Tan and Cheng 2016]. Meanwhile, the angle θ$_i$ was situated between the direction of the beam *OI* (connecting the i-th point of the point cloud with the analytical point of the scanner) and the normal vector (estimated

based on the plane fitted in the immediate vicinity of the *i*-th point) [Höfle and Pfeifer 2007]. The parameters defining the measurement geometry (R_i, θ_i) used in the intensity value correction procedure were determined as follows:

$$R_i = \sqrt{\left(x_i - x_0\right)^2 + \left(y_i - y_0\right)^2 + \left(z_i - z_0\right)^2}$$ (5)

$$\theta_i = \cos^{-1}\left(\left\|\frac{\overrightarrow{OI} \cdot \overrightarrow{n_\iota}}{\left|\overrightarrow{OI}\right| \cdot \left|\overrightarrow{n_\iota}\right|}\right\|\right)$$ (6)

In the equation (6), $\overrightarrow{n_\iota} = (n_{1i}, n_{2i}, n_{3i})$ is a normal vector the surface. The incident laser beam vector $\overrightarrow{OI} = (x_i - x_0, y_i - y_0, z_i - z_0)$ is calculated on the basis of the original 3D coordinates (x_i, y_i, z_i) of the *i*-th *I* point and the coordinates (x_0, y_0, z_0) of the centre of the scanner *O*.

In accordance with the proposition of correcting raw point clouds [Fang et al. 2014], the analyses made use of the observations obtained from individual measurement positions. The various stages of the developed solutions were presented on six test fields, representing representative sections of the considered shell, situated along the structure, predisposing the analysis of the impact of measurement geometry (numbering from the top – test field No. 1–3). The scope of the conducted analyses encompassed two priority research directions: the detection of shell perforations with moisture seepage (research area A) and the identification of repaired surface fragments (research area B).
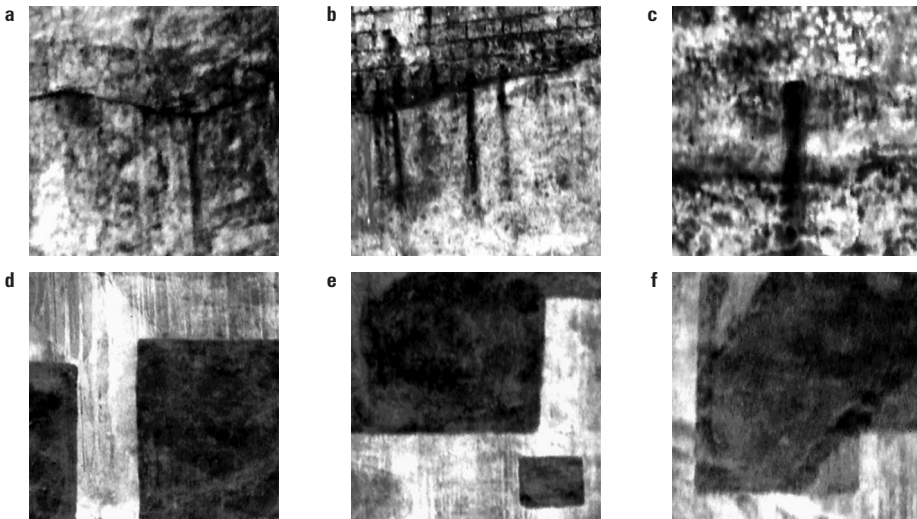
Source: Author's own study

Fig. 2. Corrected and standardised intensity values: **a**. Test field 1A; **b**. Test field 2A; **c**. Test field 3A; **d**. Test field 1B; **e**. Test field 2B; **f**. Test field 3B

The data obtained by the Z + F 5010 laser scanner, providing fourth coordinate values in the range of 1500 to 5,000,000 (in the dedicated *Z+F Laser Control* software, .zfs format), was subject to standardisation in *Cyclone* software, bringing intensity values into the range of 0 to 1, where 0 is the minimum possible value of the fourth coordinate, and 1 represents the maximum value [Fang et al. 2014, Suchocki et al. 2016]. The corrected and normalised intensity value of the laser beam reflectance, expressed on a scale of 0–1, was used for further analyses (Fig. 2).

2.3. Unsupervised classification

To automate the process of interpreting the intensity values, a common approach based on image classification techniques was employed, ensuring the grouping of pixels (per-pixel method) into relatively homogeneous clusters (cluster analysis) based on similarity expressed through spectral properties [Crespo et al. 2010, Zaczek-Peplinska et al. 2012]. Unsupervised classification of raster representations of the fourth coordinate values was preceded by an analysis of the suitability of existing algorithms for specific applications. The study of the research literature resulted in the selection of three algorithms potentially useful in the considered application: K-means, Fuzzy K-means, and ISODATA (Iterative Self-Organizing Data Analysis Technique) [Armesto-González et al. 2010; Mitka et al. 2016; Crespo et al. 2010].

Due to the relatively consistent results of all algorithms and the necessary initialisation specifying *a priori* the final number of classes, the K-means algorithm was rejected. The difficulties in selecting appropriate initial parameters for the ISODATA algorithm, and determining the outcome of unsupervised classification [Mitka et al. 2016], also led to the exclusion of this solution. The study utilised the Fuzzy K-means algorithm, considered the most reliable, enabling effective detection of areas of rising damp and other material properties [Mitka et al. 2016; Armesto-González et al. 2010].

The applied clustering algorithm – Fuzzy K-means [Bezdek 1981] – is an extension of the K-means algorithm. It replaces the definitions of the total membership of a pixel to one of the clusters with the probabilistic likelihood of the pixel belonging to each class [Ghosh and Dubey 2013]. The idea of searching for data clusters close to each other while being simultaneously distant from other points belonging to other clusters implies the iterative minimisation of the mean square classification error, which is a function of the Euclidean distance of a given pixel from the centre of the cluster [González-Jorge et al. 2012]:

$$I = \sum_{j=1}^{k} \sum_{i=1}^{n} u_{ij}^{m} \left\| x_i^{j} - c_j \right\|^2 \quad 1 \le m \le \infty \tag{7}$$

The probabilistic likelihood (u) of the corresponding image pixel (x) belonging to each cluster was based on the Euclidean distance function: pixel (x) – cluster centre (c). The algorithm initially randomly defines the k cluster centres in the pixel space, each being a weighted centroid, representing the derivative of the probability function [Chang et al. 2011]. Classifying n image pixels into the nearest of the k clusters (in

two-dimensional space) solves the problem of determining k clusters in such a way that minimises the mean square distance of each data pixel to the nearest cluster centre (c) [Mitka et al. 2016]. Using the assigned pixels to clusters, the algorithm recalculates cluster centres until the convergence criterion is met, which is that the results of successive iterations do not change [Ghosh and Dubey 2013].

Unsupervised classification of the raster representation of laser beam reflectance intensity values using the per-pixel method was conducted using tools from the PCI Geomatica package, providing the implementation of the Fuzzy K-means algorithm. The TIFF format (Tagged Image File Format) of the images of the corrected and normalised fourth coordinate values in gray-scale (generated in Cyclone) was changed to a format acceptable to the package tools (PCIDSK format). Each image pixel was assigned 8 bits, representing one of $2^8 = 256$ colours (from white through grey to black). The images were analysed automatically by extracting groups of pixels with similar reflectance properties. In order to find the appropriate number of clusters, the Fuzzy K-means function was implemented several times, changing the initial parameters of the algorithm [Kubik et al. 2008]. On the basis of the generated images, which provide a visual representation of classification results (labelling each point with a colour corresponding to the cluster to which it was assigned), the number of classes was experimentally determined to reflect the strong correlation between the fourth coordinate value and the dampness and material properties of the surface. Effective detection of rising damp on the shell (research area A) required seven classes to be extracted, while the indication of repaired surface fragments (research area B) required only two (Fig. 3).
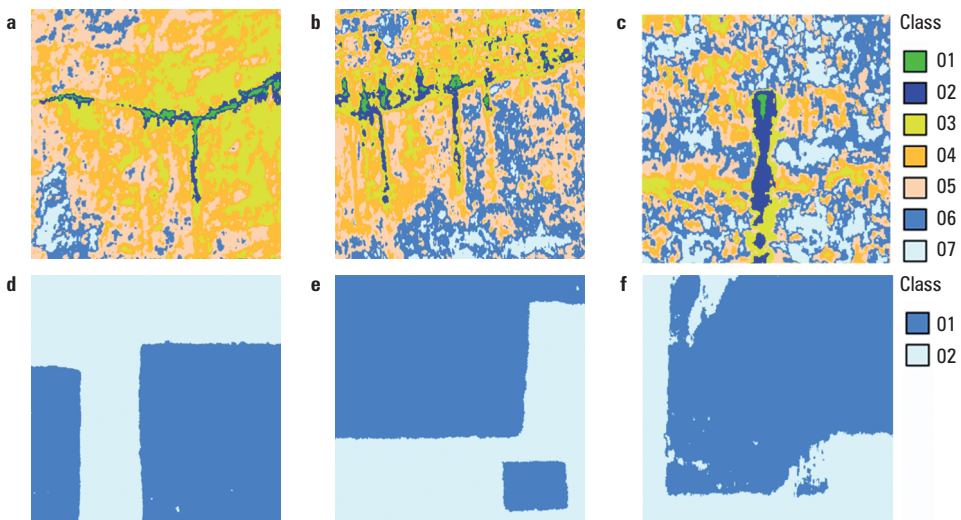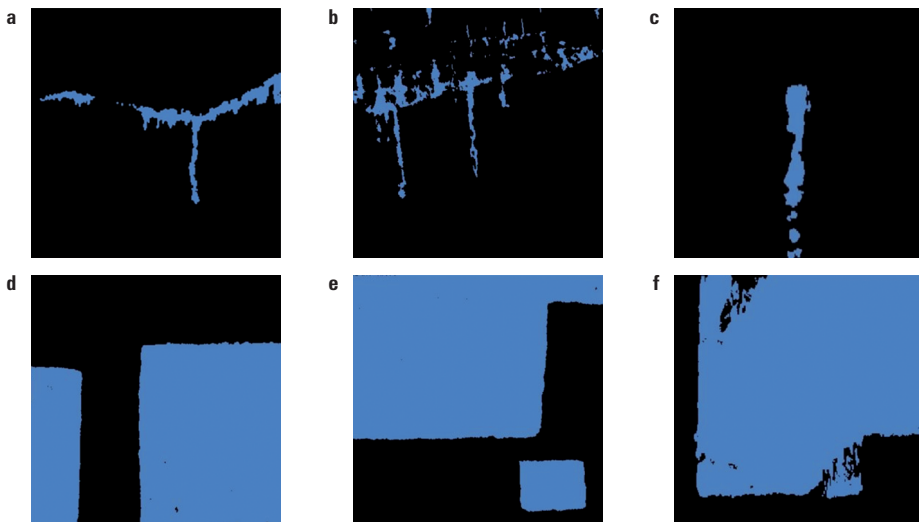

Source: Author's own study

Fig. 3. Results of unsupervised classification: **a**. Test field 1A; **b**. Test field 2A; **c**. Test field 3A; **d**. Test field 1B; **e**. Test field 2B; **f**. Test field 3B

2.4. Segmentation and vectorisation of scalar fields

As an alternative to image classification techniques, an approach eliminating information losses (resulting from the conversion of three-dimensional data into 2D images) was proposed – the segmentation of scalar fields (SF), representing corrected and normalised values of the fourth coordinate. The procedure implemented in the CloudCompare software, associating specific values of with individual points of the point cloud, involved extracting damp areas and repaired shell fragments by filtering values within experimentally established boundary ranges. Damp areas (research area A) and repaired shell fragments (research area B) were characterised by the lowest laser beam reflectance intensity values. An increase in surface dampness caused a drastic decrease in reflectance intensity compared to dry material, and similarly, repair mortar, absorbing a greater part of the laser beam, exhibited lower reflectance intensity than the unrepaired shell. The determined appropriate ranges for the corrected and normalised values of the fourth coordinate (0–0.14 and 0.15–0.225) for research areas A and B allowed for the unambiguous extraction of all points of the cloud representing moisture seepage regions and surface repair areas (Fig. 4).

Source: Author's own study

Fig. 4. Results of the filtration of scalar field values – : **a**. Test field 1A; **b**. Test field 2A; **c**. Test field 3A; **d**. Test field 1B; **e**. Test field 2B; **f**. Test field 3B

Additionally, the implementation of a strategy based on scalar fields representing the intensity values of laser beam reflectance, indicating material changes resulting from fragmentary repairs to the structure, allowed for the assessment of the quality and durability of the performed work. It also enabled metric determination of the repaired areas of the shell (preparing the verification of the quantity of used repair mortar).

The extraction of areas representing the results of repairs to individual damages was facilitated by the Connected Component Labeling (CCL) method. Initially designed for binary image classification [Samet and Tamminen 1988], the CCL algorithm is currently successfully employed for point cloud segmentation [Trevor et al. 2013]. It assigned unique labels to points in the nearest neighbourhood, facilitating the extraction of distinct, consistent components representing individual surface repair areas. The operation of the CCL algorithm required setting parameters specifying the analysis detail through the appropriate level of octree structure (o), determining the minimum distance between neighbouring components, and the minimum number of points per component (p), below which sets of points were ignored. Assuming adaptively determined parameter values ($o = 8$, $p = 10$), the cloud points were assigned appropriate labels, allowing the extraction of coherent components representing the different repair areas, marked with different colours. The consistent point sets extracted by the CCL algorithm, representing individual fragments of the shell covered with repair mortar, were vectorised using the convex hull method, applicable both in 2D and 3D space [De Berg et al. 2000]. The convex hull of a point set in 2D is the smallest convex polygon containing points on the boundary and within the set [Barber et al. 1996]. However, implementing a computationally efficient and fast method would entail significant shape generalisation, limiting the accuracy of estimating repair surface areas. In order to detail the contour of the repaired shell areas and increase the precision of the estimation of their extent, an additional parameter limiting the maximum edge length of the hull was introduced, effectively eliminating the problem of over-generalisation. The vectorised fragments of the shell covered with repair mortar, obtained using the convex hull, were exported to the DXF (Data Exchange Format) format, making it possible to estimate the repaired area (which determines the cost of the works carried out), to verify the reasonableness of repairing specific fragments of the structure and to freely share the results obtained.

3. Results

The reliability of radiometric data in assessing the condition of the reinforced concrete shell of the cooling tower, as well as the validity and effectiveness of the corrective solutions derived from the research literature, were examined based on widely applied image classification techniques. The results of the classification of representative sections of the shell – images of test fields where the colours of pixels indicated membership in the respective classes – confirmed the connection between the fourth coordinate value and the properties of the scanned surface (Fig. 4). Areas of dampness and repaired sections of the shell were characterised by the lowest intensity values of the laser beam reflectance corresponding to classes 01 and 02 (research area A) and class 01 (research area B). Tests for heterogeneity of the results obtained for representative sections of the shell were conducted based on classification reports specifying the average brightness value and standard deviation of colours in the extracted clusters. These tests took into consideration the consistency of descriptive parameters of individual classes (Table 1). The

verification based on estimators, providing only a certain estimate of parameters of the general population, was supplemented with an analysis of the significance of observed differences. Using the central limit theorem, confidence intervals were constructed at the significance level $q = 0.05$ for the average values of classes 01A, 02A, 01B, of the six test fields, and their mutual overlap was verified, giving no grounds for rejecting the hypothesis of uniformity. The overlapping confidence intervals P of average values, shown in the error estimator charts (Fig. 5) plotted in the PQStat program, allowed for the exclusion of significant differences in mean values, at a confidence level of $\alpha = 0.95$, confirming the reliability of radiometric data in assessing the condition of the concrete shell of the cooling tower, as well as the validity and effectiveness of corrective solutions derived from the research literature.

Table 1. Statistical parameters of the distributions of the intensity values of research areas A and B

Class	Test field											
	1A		2A		3A		1B		2B		3B	
	$\bar{x}$	σ	$\bar{x}$	σ	$\bar{x}$	σ	$\bar{x}$	σ	$\bar{x}$	σ	$\bar{x}$	σ
01	159.17	2.10	159.01	2.30	159.22	2.52	181.34	2.57	181.50	2.57	181.27	2.51
02	165.78	1.72	165.69	1.92	165.96	1.74						
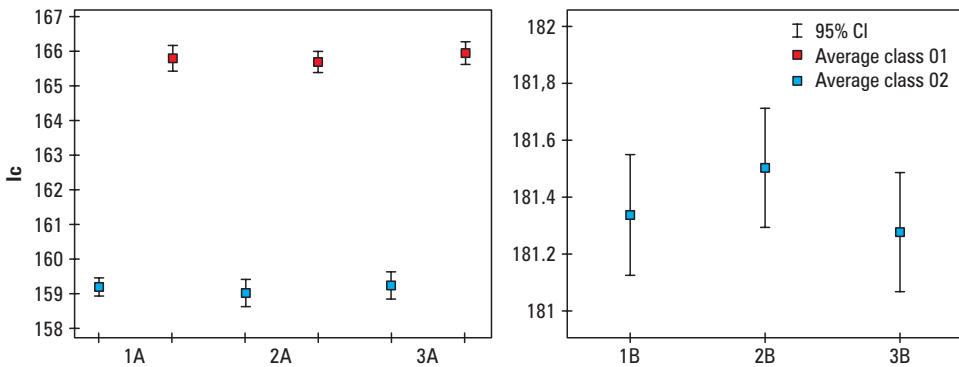
Source: Author's own study

Fig. 5. Confidence intervals of the average intensities of research areas A and B

Verification of the proposed methodology for using radiometric data as scalar fields was guaranteed by the comparison of the obtained results with the outcomes of widely applied unsupervised classification. The consistency of areas extracted based on scalar fields, representing dampness and repaired sections of the shell, with the results of image classification was verified (besides visual inspection) by considering expressed in percentages structure indices (frequencies). These indices represent the

ratios of the number of analysed units (pixels/cloud points belonging to classes 01A and 02A, as well as 01B) to the total number of the statistical population (all pixels/cloud points belonging to specific test fields). A relative index of structure similarity (Z) was applied to compare the structures resulting from the Fuzzy K-means algorithm and scalar field segmentation. Z is defined as the ratio of the sum of smaller structure indices to the sum of larger structure indices of the compared distributions. The Z index, taking values in the range of 0–1 (where unity indicates identical structures, and zero indicates extreme dissimilarity), obtained values Z ≈ 1 for both research areas (A and B) (Table 2). Determined by the near unity values of the relative similarity indices of the structures, the agreement between the image classification results and the areas extracted based on scalar field filtering confirmed the reliability of the proposed solutions.

Table 2. Percentage structure indices and relative similarity indices of the structures of the clusters of reclassified images and filtered scalar fields

Methodology	Test field					
	1A	2A	3A	1B	2B	3B
Unsupervised classification	3.37%	5.61%	3.09%	54.35%	54.37%	65.46%
Scalar fields segmentation	3.38%	5.73%	2.95%	54.31%	54.34%	67.14%
Z	0.98			0.99		

The use of radiometric data as scalar fields provided reliable metric information, the usefulness of which was confirmed by complementing the considerations based on the analysis of the local curvature of the cold store shell (detailed discussion in the paper [Makuch and Gawronek 2020]). The surface curvature determined by the principal component analysis and transformed by the square root function ($\sqrt{N}$) enabled the effective detection of all defects, chippings, and spalls of the lagging of the reinforced concrete shell of the cooling tower. The comparison of the results of intensity value analyses with the results of curvature estimates ($\sqrt{N}$) of representative fragments of the reinforced concrete structure as scalar fields effectively supplemented the elaborated concept for assessing the state of the renovated object [Makuch 2018, Makuch and Gawronek 2020] with a significant aspect of shell perforation (Fig. 6, red colour). The detection of rising damp and corrosive leaks, correlated with micro-damages to the structure, allowed the concretisation of the degree of degradation of the hyperboloidal shell according to Chmielewski's seven-level classification [2000]. Based on the analysis of radiometric data as scalar fields, integrated with the results of the surface curvature-based analysis assessment of the shell's condition, visible damages to the research object were assigned to level III – lack of lagging on surfaces exceeding 1 m^2, with sporadic visible leaks [Chmielewski 2000]. The reliability of the proposed approach was verified by comparing the obtained results with the expert assessment of the condition

of the external shell, performed from suspended scaffolds. The challenge of recording irregularities on a monolithic surface over several hundred meters, with no permanent and clear identification marks, which limits the reliability of conventional diagnostics, determined the scope of the conducted analyses. Verification of the effectiveness of detecting perforations in the reinforced concrete shell was reduced to comparisons of the quantity and approximate location of defects. The developed solution allowed for the automatic identification of all perforations and leaks noted in the expert documentation.
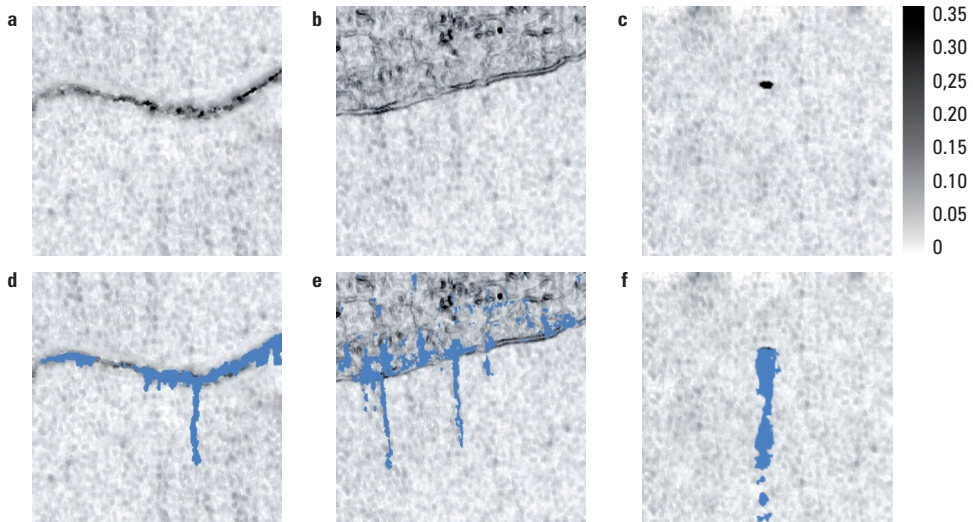
Source: Author's own study

Fig. 6. Summary of results of intensity value analyses with results of curvature estimates; Scalar field (√N): **a**. Test field 1A; **b**. Test field 2A; **c**. Test field 3A; Curvature calculation results supplemented by *Ic* segmentation results: **d**. Test field 1A; **e**. Test field 2A; **f**. Test field 3A

In addition to assessing the condition of the reinforced concrete shell, driven by the need to determine the scope of repair work, the usefulness of the proposed solutions was also considered in the context of verifying the performed surface repair. Vector data stored in the DXF format allowed for estimating the repaired surface (determining the cost of the work) and verifying the reasonableness of repairs to specific fragments of the structure by comparing the contours of damages in the shell (blue colour) extracted based on the local curvature analysis with the extent of surface repairs (red colour) (Fig. 7). The obtained results established that the analysis of intensity values as scalar fields provides an effective basis for identifying material changes characterising the repaired portions of the structure, allowing for an assessment of the validity of the work carried out and verification of the amount of repair mortar used.
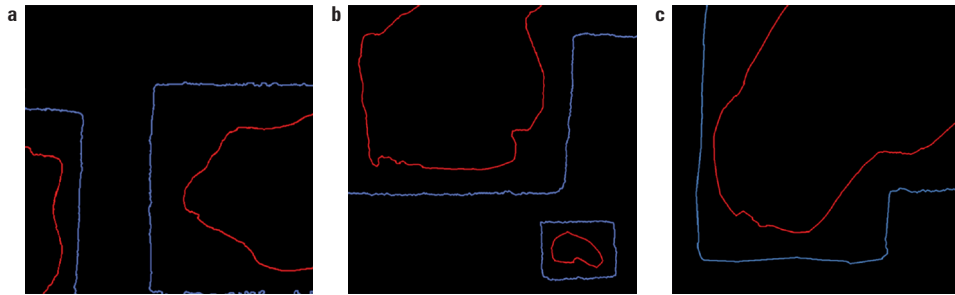
Source: Author's own study

Fig. 7. Summary results of the analyses of the extent of surface repair with damage contours.
a. Test field 1B; **b**. Test field 2B; **c**. Test field 3B

4. Conclusions

The assessment of the usefulness of laser beam reflectance intensity in diagnosing the condition of the hyperboloidal cooling tower shell was conducted on the example of a structure undergoing repairs. The empirical research, focused on detecting shell perforations and verifying repair actions, confirmed the validity of using corrected and normalised values of the fourth coordinate in these areas. An increase in surface moisture led to a dramatic decrease in reflectance intensity compared to dry material, and similarly, repair mortar, which absorbed a larger part of the laser beam, exhibited lower reflectance intensity than the unrepaired shell. The strategy proposed in the paper, which utilised radiometric information as scalar fields and eliminated information losses resulting from data conversion, proved to be a reliable alternative to commonly used image classification techniques. Scalar field segmentation, representing corrected and normalised intensity values, enabled effective detection of rising damp and corrosion leaks, complementing damage recognition based on local curvature analysis and allowing for a concrete assessment of the degradation level of the hyperboloidal shell according to a seven-point scale dictated by industry requirements. The fourth coordinate values also facilitated the identification of material changes resulting from fragmented repairs of the hyperboloidal cooling tower shell and the verification of the amount of repair mortar used. The comparison of vectorised repaired shell fragments with damage contours extracted based on local curvature analysis allowed for an assessment of the justification of the work performed.

The perspective of implementing laser beam reflectance intensity in the diagnosis of a repaired cooling tower is conditioned by adjustments to the instrument's specifications and the properties of the scanned surfaces, along with the procedures for eliminating the influence of measurement geometry. The dimensions of the hyperboloidal structure, which make it impossible to perform observations while keeping the incidence angles of the laser beam and the scanner-object distance constant (without using additional scaffolding), necessitate modifications to the fourth coordinate value.

Practical correction recommendations drawn from the research literature, based on dependencies defined in the laser equation, allowed for the effective elimination of the influence of measurement geometry, bringing the fourth coordinate values into a form corresponding to the properties of the scanned surface. However, it should be noted that the applied procedures for modifying radiometric data (conditioned by the technical specifications of the instrument and the surface properties of the observed objects) do not represent universal solutions. In the case of different technical parameters of the scanner or measurement geometry requiring the elimination of the proximity effect, they may prove ineffective. Additionally, in correcting the intensity of the research material, it was assumed that the reinforced concrete shell of the cooling tower approximately meets the roughness criterion, characterised by diffuse reflectance according to Lambert's law. Considering the real properties of the scanned surface and modifying the Lambertian reflectance model used in correction (appropriate for perfectly diffusing surfaces) could positively impact the effectiveness of the proposed solutions.

Due to the undeniable dissonance between the dimensions of the research object and the parameters of currently constructed hyperboloidal structures (for example, the tallest cooling tower in Poland at the Kozienice Power Plant has a height of 185.1 m), the priority direction for further research should be case studies illustrating the practical application of laser beam reflectance intensity and curvature analyses in assessing objects with larger geometric parameters. In this context, analyses of the suitability of the latest models of terrestrial laser scanners are planned in particular, as well as discussions of the possible necessity and economic viability of using additional rises, lifts or scaffolding. The intended direction for further work also includes laboratory studies aimed at developing an empirical correction model for intensity values, adjusted to specific instruments and the properties of the scanned surface. Additionally, efforts are envisaged to develop a comprehensive system for defining threshold values, ensuring full automation of data segmentation. There are also plans to publish papers regarding the usefulness of terrestrial laser scanning in studying the geometry of hyperboloidal cooling towers (analysing deflection, ovalisation, and geometric imperfections of structures, as well as assessing the distribution of the thickness of the concrete shell, considering any changes resulting from repairs and reinforcements) and constructing a diagnostic model that accurately reflects the behaviour of the object under actual operating conditions. Numerical simulations, considering not only basic loads but also material and geometric nonlinearity of the hyperboloidal shell, will be implemented to clarify the nature of damages and deformations of the structure. These simulations will be considered as the basis for developing an appropriate scope of interventions within the construction management system.

References

Anil E.B., Akinci B., Garrett J.H., Kurc O. 2013. Characterization of Laser Scanners for Detecting Cracks for Post-earthquake Damage Inspection. Proceedings of International Symposium on Automation and Robotics in Construction and Mining, Montreal, Canada, 313–320.

Antoniszyn K., Hawro L., Konderla P., Kutyłowski R. 2016. Wybrane problemy procesów modernizacji i remontów chłodni kominowych. Materiały Budowlane, 5 (525), 24–25.

Armesto-González J., Riveiro-Rodríguez B., González-Aguilera D., Rivas-Brea M.T. 2010. Terrestrial laser scanning intensity data applied to damage detection for historical buildings. Journal of Archaeological Science, 37(12), 3037–3047.

Bamu P.C., Zingoni A. 2005. Damage, deterioration and the long-term structural performance of cooling-tower shells: A survey of developments over the past 50 years. Engineering Structures, 27, 12, Elsevier, 1794–1800.

Barber C.B., Dobkin D.P., Huhdanpaa H. 1996. The Quickhull Algorithm for Convex Hulls. ACM Transactions on Mathematical Software, 22(4), 469–483.

Bezdek J.C. 1981. Pattern recognition with fuzzy objective function algorithms. Plenum Press, New York.

Blaskow R., Schneider D. 2014. Analysis and correction of the dependency between laser scanner intensity values and range. The International Archives of the Photogrammetry, Remote Sensing and Spatial Information Sciences, XL-5, ISPRS Technical Commission V Symposium, Riva del Garda, Italy.

Buczek M., Paszek M., Szafarczyk A. 2018. Application of Laser Scanning for Creating Geological Documentation. E3S Web Conf., 35, 04001.

Camp G., Carreaud P., Lançon H. 2013. Large Structures: Which Solutions For Health Monitoring? International Archives of the Photogrammetry, Remote Sensing and Spatial Information Sciences, XL-5/W2. XXIV International CIPA Symposium, Strasbourg, France.

Chang C.T., Lai J.Z.C., Jeng M.D. 2011. A Fuzzy K-means Clustering Algorithm Using Cluster Center Displacement. Journal of Information Science and Engineering, 27, 995–1009.

Chen X., Li J.A. 2016. Feasibility Study on Use of Generic Mobile Laser Scanning System for Detecting Asphalt Pavement Cracks. ISPRS Remote Sensing and Spatial Information Sciences, XLI-B1, 545–549.

Chmielewski T. 2000. O niezawodności chłodni kominowych. II Konferencja Naukowo-Techniczna „Problemy eksploatacji, remontów i wznoszenia budowlanych obiektów energetycznych". Prace Naukowe Instytutu Budownictwa Politechniki Wrocławskiej, 78, Wrocław, 35–40.

Crespo C., Armesto J., González-Aguilera D., Arias P. 2010. Damage detection on historical buildings using unsupervised classification techniques. International Archives of Photogrammetry, Remote Sensing and Spatial Information Sciences, XXXVIII. Part 5 Commission V Symposium, Newcastle upon Tyne, UK, 184–188.

Erkal B.G., Hajjar J.F. 2017. Laser-based surface damage detection and quantification using predicted surface properties. Automation in Construction, 83, 285–302.

Fang W., Huang X., Zhang F., Li D. 2014. Intensity Correction of Terrestrial Laser Scanning Data by Estimating Laser Transmission Function. IEEE Transactions on Geoscience and Remote Sensing, 1–10.

Franceschi M., Teza G., Preto N., Pesci A., Galgaro A., Girardi S. 2009. Discrimination between marls and limestones using intensity data from terrestrial laser scanner. ISPRS Journal of Photogrammetry and Remote Sensing, 64, 522–528.

García-Talegón J., Calabrés S., Fernández-Lozano J., Iñigo A. C., Herrero-Fernández H., Arias-Pérez B., González-Aguilera D. 2015. Assessing pathologies on Villamayor Stone (Salamanca, Spain) by terrestrial laser scanner intensity data. Int. Arch. Photogramm. Remote Sens. Spatial Inf. Sci., XL-5/W4, 445–451.

Gawronek P., Noszczyk T. 2023. Does more mean better? Remote-sensing data for monitoring sustainable redevelopment of a historical granary in Mydlniki, Kraków. Herit. Sci., 11, 23.

Ghosh S., Dubey S.K. 2013. Comparative Analysis of K-Means and Fuzzy C-Means Algorithms. International Journal of Advanced Computer Science and Applications, 4, 4, 35–39.

González-Jorge H., Gonzalez-Aguilera D., Rodriguez-Gonzalvez P., Arias P. 2012. Monitoring biological crusts in civil engineering structures using intensity data from terrestrial laser scanners. Construction and Building Materials, 31, 119–128.

Gradka R., Kwinta A. 2017. Wyznaczenie mapy deformacji obiektu inżynierskiego. Archiwum Fotogrametrii, Kartografii i Teledetekcji, 29, 49–62.

Hancock C.M., Roberts G.W., Bisby L., Cullen M., Arbuckle J. 2012. Detecting fire damaged concrete using laser scanning. Proceedings of FIG Working Week, Rome, Italy.

Höfle B., Pfeifer N. 2007. Correction of laser scanning intensity data: Data and model-driven approaches. ISPRS Journal of Photogrammetry and Remote Sensing, 62(6), 415–433.

Humair F., Abellan A., Carrea D., Matasci B., Epard J.L., Jaboyedoff M. 2015. Geological layers detection and characterisation using high resolution 3D point clouds: example of a box-fold in the Swiss Jura Mountains. European Journal of Remote Sensing, 48, 1, 541–568.

Ioannidis C., Valani A., Georgopoulos A., Tsiligiris E. 2006. 3D model generation for deformation analysis using laser scanning data of a cooling tower. 3rd IAG/12th FIG Symposium, Baden, 22–24.

Jawański W., Stefanek K. 2011. Remonty chłodni kominowych – 20 lat technologii firmy Sika w Polsce. Awarie Budowlane, XXV Konferencja Naukowo-Techniczna, Międzyzdroje, 337–348.

Kaasalainen S., Jaakkola A., Kaasalainen M., Krooks A., Kukko A. 2011. Analysis of incidence angle and distance effects on terrestrial laser scanner intensity: Search for correction methods. Remote Sensing, 3, 2207–2221.

Kashani A.G., Olsen M.J., Parrish C.E., Wilson N. 2015. A Review of LIDAR Radiometric Processing: From Ad Hoc Intensity Correction to Rigorous Radiometric Calibration. Sensors, 15, 28099–28128.

Kocierz R., Ortyl Ł., Kuras P., Owerko T., Kędzierski M. 2016. Geodezyjne metody pomiarowe w diagnostyce obiektów budownictwa energetycznego. Materiały Budowlane, 5, 525.

Krooks A., Kaasalainen S., Hakala T., Nevalainen O. 2013. Correcting of intensity incidence angle effect in terrestrial laser scanning. ISPRS Annals of the Photogrammetry, Remote Sensing and Spatial Information Sciences, II-5/W2, 145–150.

Kubik T., Paluszyński W., Iwaniak A., Tymków P. 2008. Klasyfikacja obrazów rastrowych z wykorzystaniem sztucznych sieci neuronowych i statystycznych metod klasyfikacji. Monografia. Wydawnictwo Uniwersytetu Przyrodniczego we Wrocławiu.

Kwinta A., Bac-Bronowicz J. 2021. Analysis of hyperboloid cooling tower projection on 2D shape. Geomatics, Landmanagement and Landscape, 3, 25–40.

Laefer D.F., Gannon J., Deely E. 2010. Reliability of crack detection methods for baseline condition assessments. Journal of Infrastructure Systems, 16(2), 129–137.

Lerones P.M., Vélez D.O., Rojo F.G., Gómez-García-Bermejo J., Casanova E.Z. 2016. Moisture detection in heritage buildings by 3D laser scanning. Studies in Conservation, 61, supl., 46–54.

Li Q., Cheng X. 2018. Damage Detection for Historical Architectures Based on TLS Intensity Data. ISPRS Remote Sensing and Spatial Information Sciences, XLII-3, 915–921.

Makuch M. 2018. Application of terrestrial laser scanning in the process of modernization of hyperboloid cooling towers. Faculty of Environmental Engineering and Land Surveying, University of Agriculture in Krakow (PhD thesis). Krakow (in Polish).

Makuch M., Gawronek P. 2020. 3D Point Cloud Analysis for Damage Detection on Hyperboloid Cooling Tower Shells. Remote Sensing, 12(10), 1542.

Mills J., Barber D. 2003. An Addendum to the Metric Survey Specifications for English Heritage. The collection and archiving of point cloud data obtained by terrestrial laser scanning or other methods. The Metric Survey Team, York.

Mitka B., Makuch M., Gawronek P. 2016. Zastosowanie intensywności wiązki odbicia w ocenie stanu powierzchni budowli zabytkowych. Episteme, 32, 11–24.

Mosalam K.M., Takhirov S.M., Park S.T. 2014. Applications of laser scanning to structures in laboratory tests and field surveys. Structural Control and Health Monitoring, 21, 115–134.

Mukupa W., Roberts G.W., Hancock C.M., Al-Manasir K. 2016. A non-destructive technique for health assessment of fire-damaged concrete elements using terrestrial laser scanning. Journal of Civil Structural Health Monitoring, 6(1), 1–15.

Olsen M.J., Kuester F., Chang B.J., Hutchinson T.C. 2010. Terrestrial laser scanning-based structural damage assessment. Journal of Computing in Civil Engineering, 24(3), 264–272.

Pfeifer N., Dorninger P., Haring A., Fan H. 2007. Investigating terrestrial laser scanning intensity data: quality and functional relations. 8th Conference on Optical 3-D Measurement Techniques, 328–337.

Piot S., Lançon H. 2012. New Tools for the Monitoring of Cooling Towers. 6th European Workshop on Structural Health Monitoring. 6th European Workshop on Structural Health Monitoring (EWSHM 2012), July 3–6, 2012.

Samet H., Tamminen M. 1988. Efficient Component Labeling of Images of Arbitrary Dimension Represented by Linear Bintrees. IEEE Transactions on Pattern Analysis and Machine Intelligence, 10 (4), 579–586.

Soudarissanane S., Lindenbergh R., Menenti M., Krooks A., Kukko A. 2011. Scanning geometry: Influencing factor on the quality of terrestrial laser scanning points. ISPRS Photogrammetry, Remote Sensing, 66, 389–399.

Suchocki C., Damięcka-Suchocka M., Katzer J. 2016. Wpływ czynników na wartość siły odbicia wiązki lasera w naziemnym skaningu laserowym. Wybrane prace naukowe zespołów badawczych prowadzone na kierunku Geodezja i Kartografia. Monografia z okazji 15-lecia kierunku Geodezja i Kartografia na Politechnice Koszalińskiej, Koszalin, 5–21.

Tan K., Cheng X. 2016. Correction of Incidence Angle and Distance Effects on TLS Intensity Data Based on Reference Targets. Remote Sensing, 8, 251–271.

Toś C. 2013. Supervised classification of laser scanning data in the assessment of technical conditions of masonry constructions. Technical transactions, Environment engineering 1-Ś/2013, 131–141.

Trevor A.J., Gedikli S., Rusu R.B., Christensen H.I. 2013. Efficient organized point cloud segmentation with connected components. Semantic Perception Mapping and Exploration.

Tsai Y.C.J., Li F. 2012. Critical assessment of detecting asphalt pavement cracks under different lighting and low intensity contrast conditions using emerging 3D laser technology. Journal of Transportation Engineering, 138(5), 649–656.

Voegtle T., Schwab I., Landes T. 2008. Influences of different materials on the measurements of a terrestrial laser scanner (TLS). Proc. of the XXI Congress. The International Society for Photogrammetry and Remote Sensing, ISPRS2008, Beijing, China, July 3–11, 2008, 1061–1066.

Xu X., Yang H., Neumann I. 2015. Concrete Crack Measurement and Analysis Based on Terrestrial Laser Scanning Technology. Sensors & Transducers, 186, 3, 168–172.

Zacharopoulou A., Zacharopoulou E., Batis G. 2013. Statistics Analysis Measures Painting of Cooling Tower. International Journal of Corrosion. Article ID 389159.

Zaczek-Peplinska J., Osińska-Skotak K., Gergont K. 2012. Możliwości wykorzystania zmian intensywności odbicia promienia laserowego do oceny stanu konstrukcji betonowej. In: Inżynieryjne zastosowania geodezji. Wydawnictwo Politechniki Poznańskiej, Poznań.

PhD Maria Makuch
University of Agriculture in Krakow
Department of Geodesy
ul. Balicka 253a, 30-198 Kraków
e-mail: maria.makuch@urk.edu.pl
ORCID:0000-0003-0578-5313